Supplementary information

Inhibition of mitochondrial dysfunction and neuronal cell death in models of Huntington's disease and in HD patients-derived cells

Xing Guo[1,#], Marie-Helene Disatnik[3,#], Marie Monbureau[4], Mehrdad Shamloo[4], Daria Mochly-Rosen[3,*] and Xin Qi[1, 2,*]

[1]Department of Physiology & Biophysics, [2] Center of Mitochondrial Disease, Case Western Reserve University School of Medicine, Cleveland, OH 44106, USA, [3]Department of Chemical and Systems Biology, Stanford University School of Medicine, Stanford, CA 94305, USA, and [4]Behavioral and Functional Neuroscience Laboratory, School of Medicine, Stanford University, Stanford, CA 94305, USA.
[#] These authors contributed equally to this work

*__Corresponding authors__:
Daria Mochly-Rosen PhD, Department of Chemical and Systems Biology, Stanford University School of Medicine, CCSR, Room 3145A, 269 Campus Dr., Stanford, California 94305, USA. Tel: 650-725-7720; Fax: 650-723-4686; E-mail: mochly@stanford.edu;
Xin Qi PhD, Department of Physiology and Biophysics, Case Western Reserve University School of Medicine, 10900 Euclid Ave, E516, Cleveland, Ohio, 44106-4970, USA. Tel: 216-368-4459; Fax: 216-368-5586; E-mail: xxq38@case.edu

Supplementary figure legend

Fig 1S: **P110-TAT treatment had no effect on the levels of Htt, Drp1 and mitochondrial fusion proteins in HD cell cultures.** (A) Mouse striatal HdhQ7 (wild-type) and HdhQ111 (mutant) cells were treated with TAT or P110-TAT (P110; each at 1 μM) for 3 days. (B) Wild-type mouse striatal cells were treated with 3-NP (5 mM) for 4 hours following 30 min incubation of P110-TAT (1 μM) treatment. (C) 293T cells were transfected with either 23Q or 73Q Htt for 48 hours in the presence of TAT or P110-TAT. Total lysates harvested from the above cells were subjected to western blot analyses with the indicated antibodies. Actin was used as a loading control. The shown blots are representative of 2-3 independent experiments.

Fig 2S: (A) Images include a number of cells in each treatment group, corresponding to the Fig. 1F. (B) Images with a number of cells in each treatment group corresponding to the Fig. 2A. (C) Images with a number of cells corresponding to the Fig. 2C. Scale bar is 10 um. (D) HdhQ111 mouse striatal cells were transfected with either control siRNA (Invitrogen, USA) or Drp1 siRNA (Thermo scientific., USA) using *Trans*IT®-2020 Transfection Reagent (Mirus Bio LLC, Madison, WI), according to manufacturer's instructions. TAT or P110-TAT (1 μM, each) was added to the cultured cells 1 day after siRNA was transfected. Two days later, cells were fixed and stained with anti-TOM20 antibody. The histogram provides quantitation of the percentage of

cells with fragmented mitochondria relative to the total number of cells; data are the mean ± S.E. of three independent experiments. At least 100 cells per group were counted. Insert: a confirmation of knock-down of Drp1 by Drp1 siRNA. *, #, $p<0.05$ vs HdhQ111 cells transfected with con siRNA and treated with TAT. (E) Mouse striatal HdhQ7 (wild-type) and HdhQ111 (mutant) cells were treated with P110-TAT (P110, 1 μM) for 3 days. Total lysates harvested from above cells were subjected to western blot analysis with anti-p53 antibodies. Actin was used as a loading control.

Fig 3S: (A) Expression of Drp1 had no effect on protein and mRNA levels of p53 in mouse striatal wild-type cells. Myc-Drp1 or control vector were expressed in mouse wild-type striatal cells. Total protein levels of p53 were determined by western blot analysis. Actin was used as a loading control. p53 mRNA levels were determined by RT-PCR, and GAPDH was an internal control. Primers were shown in Suppl. Table 1. **(B) Expression of p53 did not induce Drp1 translocation to the mitochondria.** GFP or GFP-p53 (6 μg for each) were expressed in mouse wild-type striatal cells or p53-null H1299 cells. Mitochondrial fractions were isolated, and Drp1 mitochondrial levels were determined by western blot analysis. VDAC was used as a loading control. Shown are representative data from two independent experiments. **(C) Expression of p53 had no effect on Drp1 total protein level.** GFP (4 μg) or GFP-p53 (2 and 4 μg) were expressed in mouse wild-type striatal cells. Total protein level of Drp1 was determined by western blot analysis, and actin was used as a loading control. Shown are representative data from three independent of experiments. **(D) PFTα treatment had no effects on Drp1 and p53 translocation to the mitochondria**. HD striatal cells were treated with PFTα (5 μM), and mitochondrial fractions were isolated. Western blot analysis determined Drp1 and p53 levels in the mitochondrial fractions. Shown is a representative blot of two independent experiments. HSP60 was used as a loading control.

Fig 4S: Characterization of iPS cell lines. (A) iPS cells derived from either normal fibroblasts (nHDF) or fibroblasts from a HD patient (GM 05539) were plated on Matrigel-coated coverslips for immunostaining to determine expression of stem cell markers. The iPS cells expressed stem cell antigens including OCT4 and SOX2 (nuclei), SSEA-4 (cytoplasm) and TRA-1-60 and -81 (cell surface). Positive alkaline phosphatase (AP) is shown on the top. Phase contrast images in the bottom display typical ES-like morphology. **(B)** Con- and HD-iPS cells were subjected to EBs formation for testing *in vitro* pluripotency. After 15 days, all EBs expressed markers of mesoderm (α-SMA), ectoderm (βIII-tubulin), and endoderm (GATA-4). **(C)** Karyotype analysis of HD-iPS cells is carried out by Cell Line Genetics (Madison, Wisconsin, USA). In addition, fingerprint analysis confirmed that the alleles of HD-iPS cells matched the DNA fingerprint pattern of fibroblast GM05539.

Fig 5S: (A) Protein levels of mitochondrial dynamics-related proteins were determined by western blot analysis with the indicated antibodies. **(B)** Total lysates of Con- or HD-iPS human cells were subjected to western blot analysis with anti-Drp1 or anti-p53 antibodies. Actin was used as a loading control. Shown is a representative image of two independent experiments. **(C)** Neurons differentiated from Con-iPS cells were stained with GAD67 (green) to determine GABAergic neurons, Calbindin (green) for striatal neurons and DARPP-32 (green) for medium spiny neurons. Neuronal cells were confirmed by positive staining with anti-MAP2 or anti-TUJ1 (red). Nuclei were stained with DAPI (Blue). Because we followed the method (1) to induce

GABAergic striatal neuron differentiation stepwise, it is difficult to estimate overall percentage of striatal neurons generated from original iPS cells. The yield of GABAergic neurons was approximately 50-60% and the yield of DARPP-32 positive neurons was approximately 10-15%. Scale bar is 100 μm.

Fig 6S: (A) **P110-TAT can be delivered into neurons of mice**. Naïve mice were treated with FITC-P110-TAT (3 mg/kg/day using an Alzet mini pump) for 1 day or 14 days. The brains were harvested and sectioned. FITC labeled signal in striatum was then imaged. The bottom images are enlarged from boxed area in upper panels. Arrowhead indicates neurons with FITC peptide labeling. (B) **Peptide stability:** Peptide stability **on day** 0 and day 28 in the Alzet pump was determined by analytical HPLC and no significant change in P110-TAT stability was observed. (C) **Toxicity**: The potential toxicity of the peptide was assessed *in vivo* by the Department of Comparative Medicine at Stanford University. Histologic examination of all organs and blood cells were analyzed and no significant differences were observed between P110-TAT-treated and untreated-mice (accession # L12004753-5).

Fig 7S: P110 treatment attenuated behavior deficits in R6/2 mice. R6/2 and wild-type littermates were treated with TAT or P110-TAT (P110, 3 mg/kg/day) using Alzet osmotic pumps. Behavior analysis including Activity Chamber test to determine activity levels and Y maze (memory and recognition activity) were performed by an experimenter blind to genotype and treatment. Two separate studies (Cohorts A and B) were carried out. The behavior of R6/2 mice was tested every other week. Dot: record of individual animal; short line represents mean data of each group. P110 treatment ameliorated motor activity and cognitive activity of R6/2 mice. (A) Mice that died before the end of the testing period were excluded from statistical analysis. RM ANOVAs were run on each cohort. Cohort A: There was no significant overall difference in Total Distance moved between P110 and TAT treatment groups in R6/2 mice ($p=0.0845$; Time $p<0.0001$; Interaction Time/Treatment $p=0.1428$). Cohort B: Analyses revealed an overall significant difference between P110 and TAT treatment groups in R6/2 mice ($p=0.0211$; Time $p<0.0001$; Interaction $p=0.3677$). (B) Mice that died before the end of the testing period were excluded from statistical analysis. RM ANOVAs were run on each cohort. Cohort A: Analyses showed an overall significant difference between P110 and TAT treatment groups in R6/2 mice ($p=0.0192$; Time $p= 0.6495$; Interaction $p=0.2160$). Cohort B: Analyses showed an overall significant difference in P110 and TAT Treatment groups in R6/2 mice ($p=0.0462$; Time $p=0.3762$; Interaction $p=0.4512$).

Table 1S

	Primer
Mouse-p53-F	CCCCTGTCATCTTTTGTCCCT
Mouse-p53-R	AGCTGGCAGAATAGCTTATTGAG
Mouse-GAPDF-F	TGGCCTTCCGTGTTCCTAC
Mouse-GAPDH-R	GAGTTGCTGTTGAAGTCGCA

References:

1. Zhang, N., An, M.C., Montoro, D., and Ellerby, L.M. 2010. Characterization of Human Huntington's Disease Cell Model from Induced Pluripotent Stem Cells. *PLoS Curr* 2:RRN1193.

Suppl Fig 1

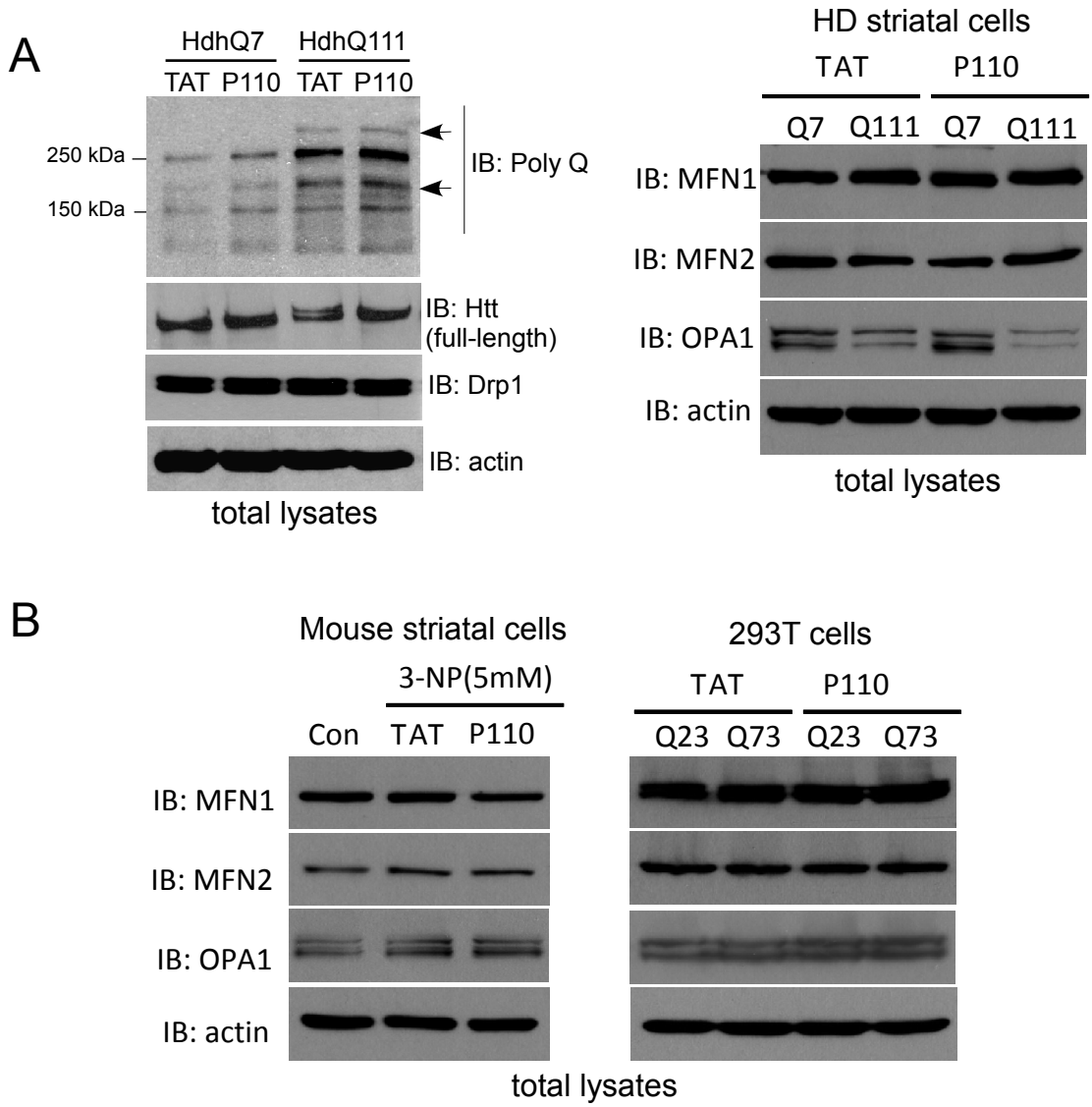
A
HdhQ7
HdhQ111
TAT P110 TAT P110
250 kDa
150 kDa
IB: Poly Q
IB: Htt (full-length)
IB: Drp1
IB: actin
total lysates
HD striatal cells
TAT
P110
Q7 Q111 Q7 Q111
IB: MFN1
IB: MFN2
IB: OPA1
IB: actin
total lysates
B
Mouse striatal cells
3-NP(5mM)
Con TAT P110
IB: MFN1
IB: MFN2
IB: OPA1
IB: actin
293T cells
TAT
P110
Q23 Q73 Q23 Q73
total lysates

Suppl Figure 2

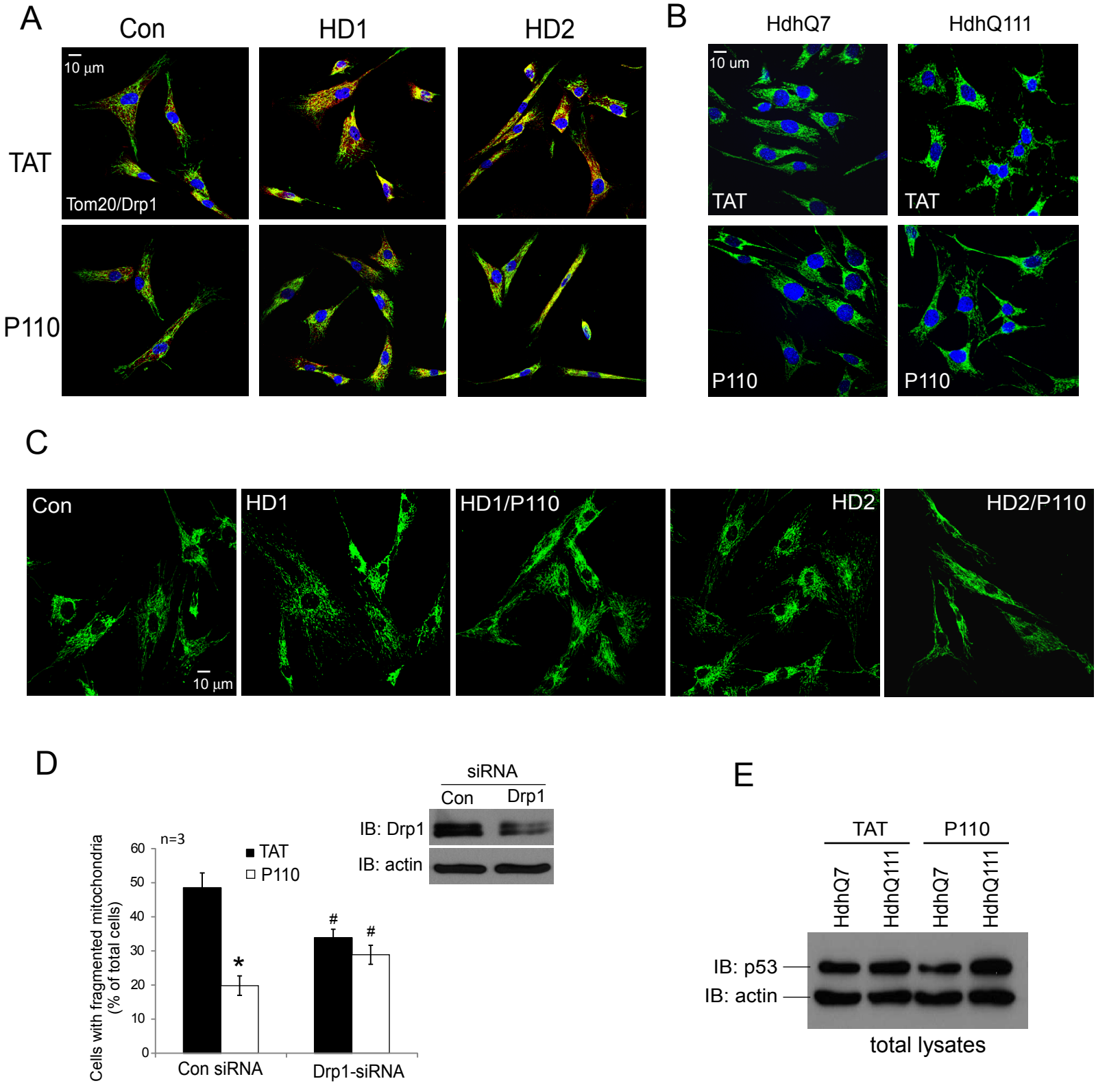

Suppl Fig 3

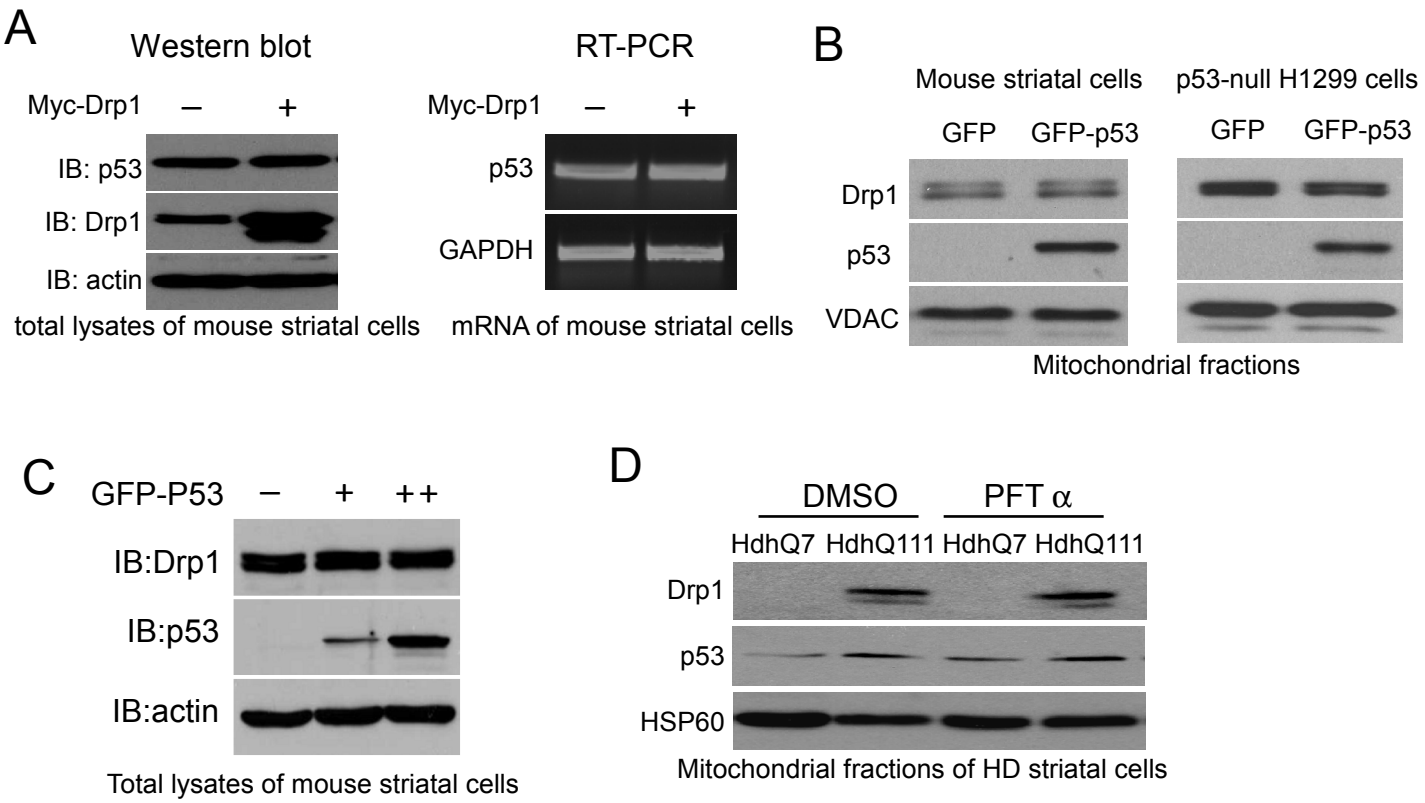
A
Western blot
Myc-Drp1 – +
IB: p53
IB: Drp1
IB: actin
total lysates of mouse striatal cells
RT-PCR
Myc-Drp1 – +
p53
GAPDH
mRNA of mouse striatal cells
B
Mouse striatal cells
p53-null H1299 cells
GFP GFP-p53
GFP GFP-p53
Drp1
p53
VDAC
Mitochondrial fractions
C
GFP-P53 – + ++
IB:Drp1
IB:p53
IB:actin
Total lysates of mouse striatal cells
D
DMSO
PFT α
HdhQ7 HdhQ111 HdhQ7 HdhQ111
Drp1
p53
HSP60
Mitochondrial fractions of HD striatal cells

Suppl Fig 4

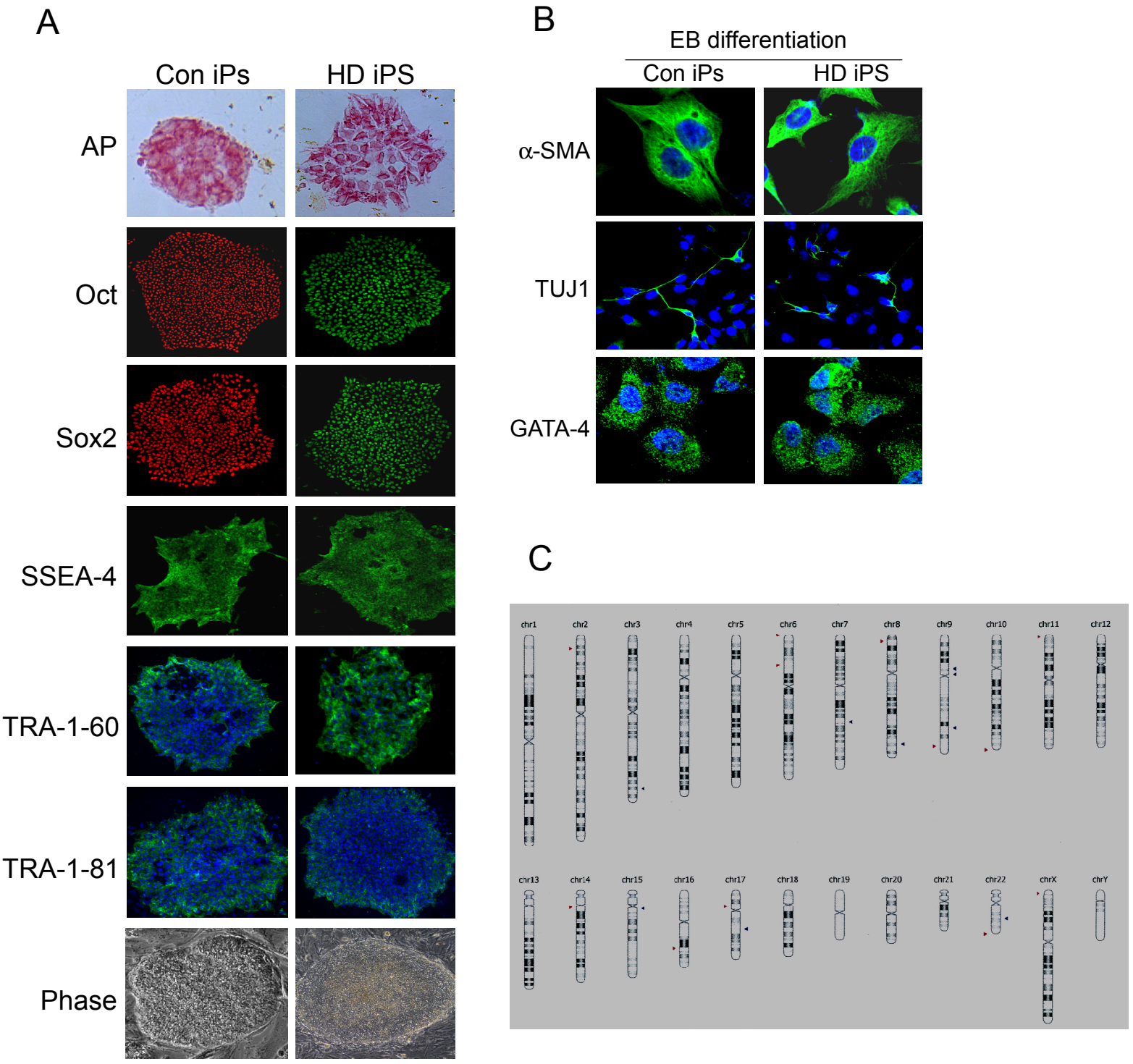

HD iPS cells and iPS cell-derived embryonic bodies

Suppl Fig. 5

A

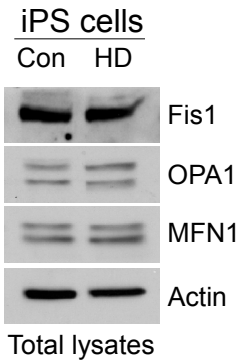

B

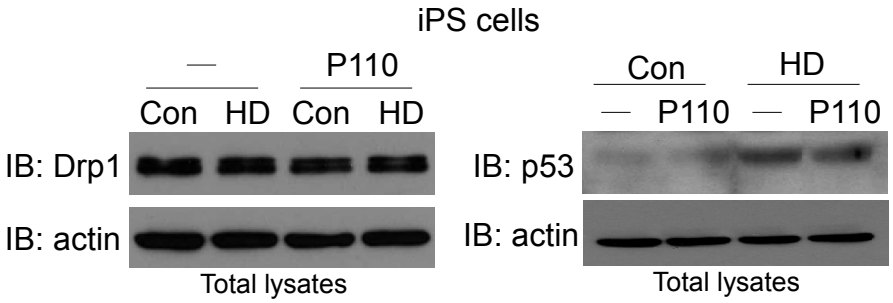

C

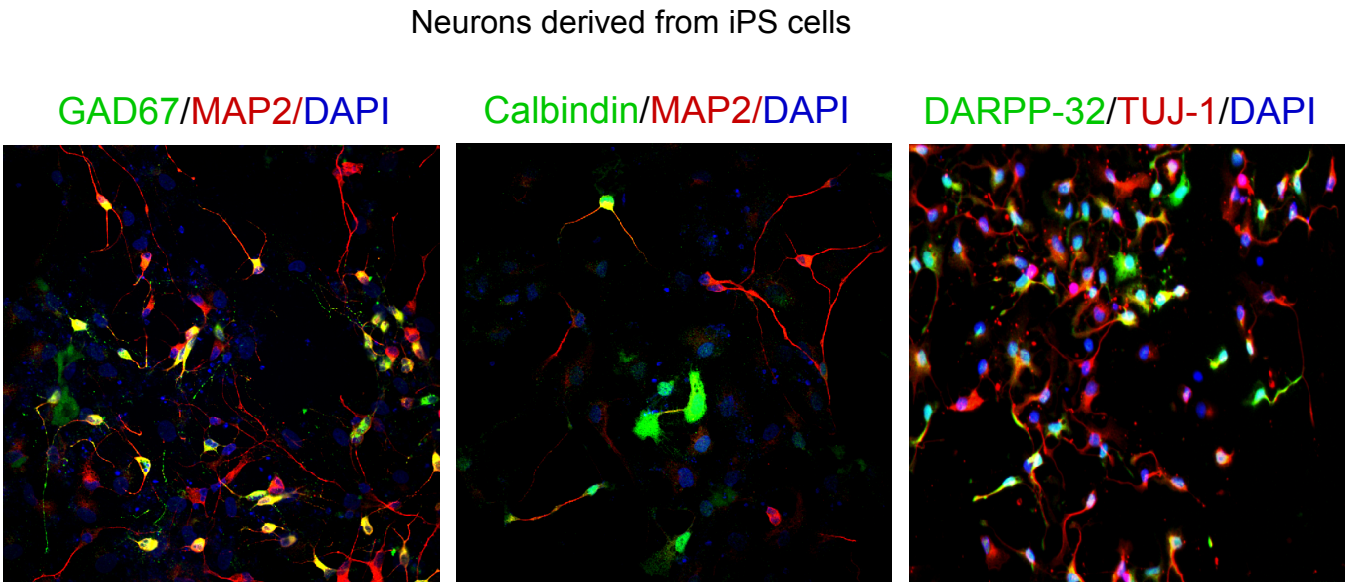

HD iPS cells and iPS cells-derived neurons

Suppl Figure 6

A

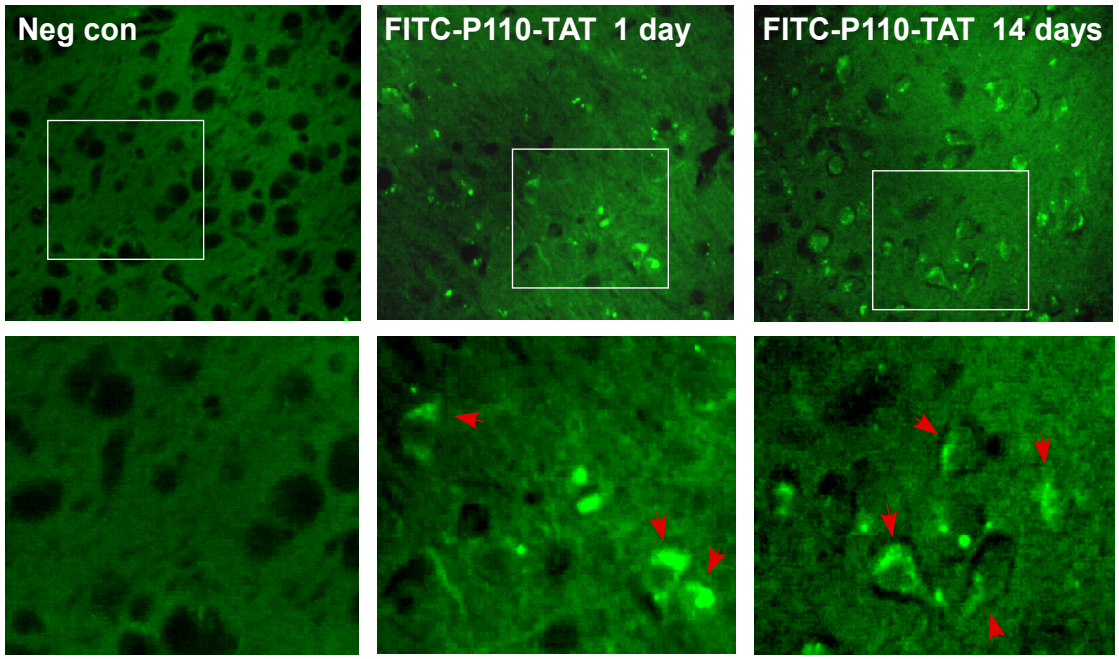

B

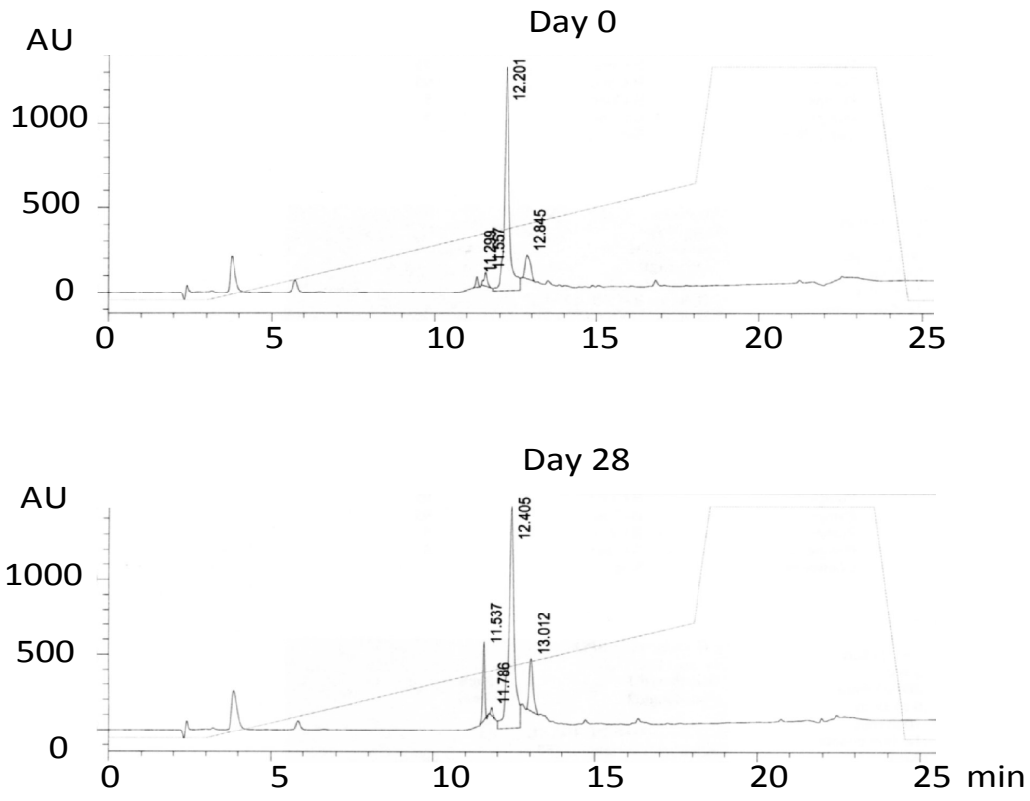

Suppl. Fig 7

A

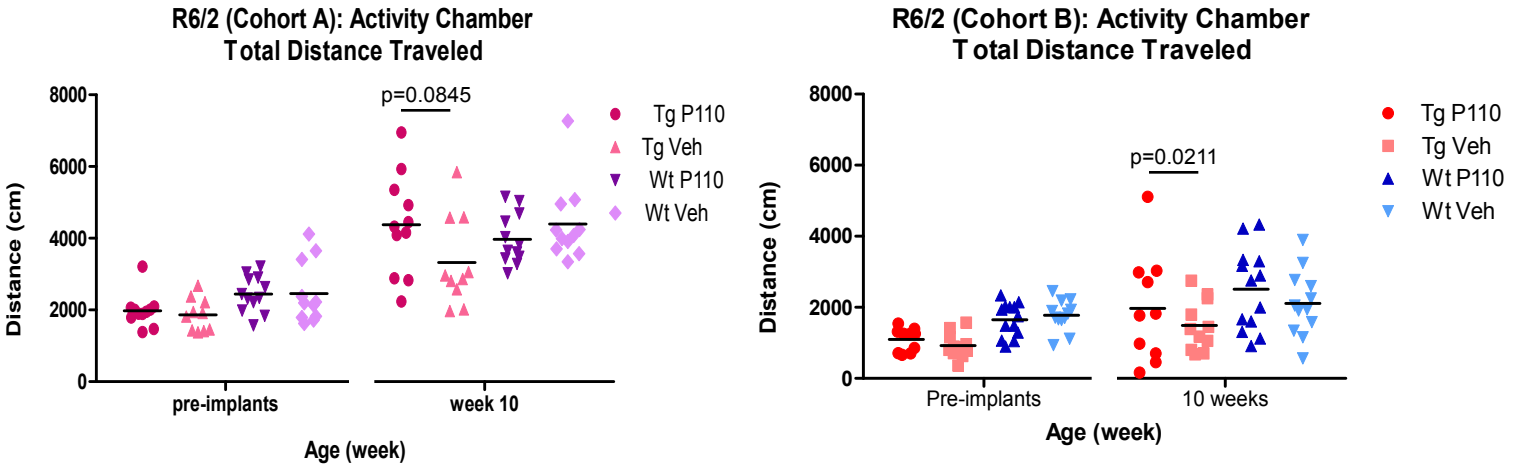

B

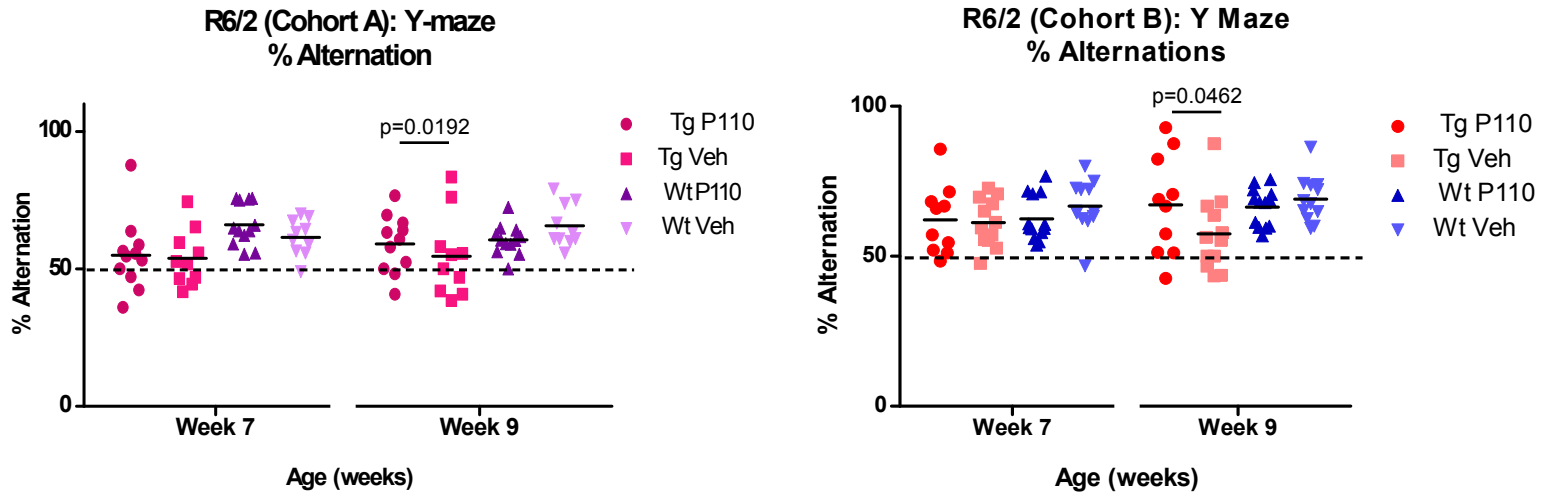

In vivo studies with R6/2 HD mice and littermates